ChemPubSoc Europe

DOI: 10.1002/chem.201702378

CHEMISTRY
A European Journal
Full Paper

Metal–Ligand Complexes

A Novel Bulky Heteroaromatic-Substituted Methanide Mimicking NacNac: Bis(4,6-*tert*-butylbenzoxazol-2-yl)methanide in s-Block Metal Coordination**

Ingo Koehne, Sebastian Bachmann, Thomas Niklas, Regine Herbst-Irmer, and Dietmar Stalke*[a]

Dedicated to Professor Dieter Fenske on the occasion of his 75th birthday

Abstract: A novel bulky bis(4,6-*t*Bu-benzoxazol-2-yl)methane ligand was synthesized in a straightforward three-step synthesis. The corresponding complexes [Li{(4,6-*t*Bu-$NCOC_6H_2)_2CH$}THF], $[K\{\eta^5\text{-}(4,6\text{-}t\text{Bu-}NCOC_6H_2)_2CH\}]_\infty$, and $[MgCl\{(4,6\text{-}t\text{Bu-}NCOC_6H_2)_2CH\}(THF)_2]$ were obtained upon metalation with alkaline or alkaline-earth-metal reagents. Reduction of $[MgCl\{(4,6\text{-}t\text{Bu-}NCOC_6H_2)_2CH\}(THF)_2]$ with potassium metal or KC_8 led to the formation of the homoleptic compound $[Mg\{(4,6\text{-}t\text{Bu-}NCOC_6H_2)_2CH\}_2]$. All compounds were fully characterized. Their solid-state structures as well as their behavior in solution, which was analyzed with the help of advanced NMR spectroscopic techniques, are discussed in detail.

Introduction

Since the introduction of the first transition-metal complexes of the versatile β-diketiminate (NacNac) ligand in 1968 this ligand platform has gained more-and-more popularity.[1–3] Due to the easy modification of the electronic and steric properties of NacNac by simply varying the substituents at the imine moieties, a variety of differently substituted derivatives can be synthesized (Scheme 1).[4,5] In this context, the Dipp (diisopropylphenyl) substituted NacNac derivative in particular has been one of the most-studied ligand systems since its first synthesis in 1997.[6–8] The phenyl groups within this system display an almost perpendicular orientation with respect to the residual imine ligand backbone, which offers unique shielding towards a coordinated metal ion and thus avoids oligomerization or electrophilic attack.[9]

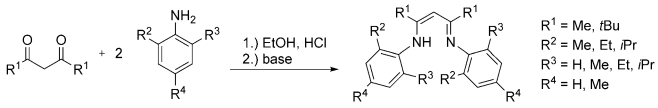

Scheme 1. Synthesis of aryl-substituted NacNacH ligands.

To further increase the bulkiness at the ligand periphery of the NacNac system, *t*Bu groups were successfully introduced by Budzelaar et al.[10] Furthermore, supersized imine residues containing *N*-terphenyl substituents could be generated.[11] With regards to modification at the bridging moiety, it was shown that a coordinating NacNac ligand cleanly reacts with diphenylketene to yield a tripodal ligated diimine-enolate complex.[12]

Consequently, in the last two decades a tremendous variety of β-diketiminate-derived main-group compounds have been synthesized and proven to be as catalytically active as transition-metal catalysts.[13–15] For example, with the alkaline-earth metals (Mg, Ca, Sr, and Ba) these complexes range from alkyl- to mono- and dimeric hydrido- and halido-substituted compounds. Remarkably, starting from this ligand platform it was also possible to access dimeric low-oxidation-state magnesium(I) complexes, which turned out to be versatile two-center two-electron reducing agents.[16–23]

This rising interest also initiated research into other promising ligand platforms that mimic the chelating ability of the ubiquitous NacNac ligand, in particular the feature that two imine nitrogen atoms function as Lewis donors to a coordinating metal ion to form a six-membered metallaheterocycle. Examples are the bis(2-pyridyl)methane ligand system and its N, P, and As bridged derivatives with benzo-fused imine moieties (Scheme 2, left).[24–33] Furthermore, a new ligand class arose when the 2-pyridyl residues were exchanged for benzannulated oxazoline sidearms. Despite the fact that bis(heterocyclo)-methane ligands (L) can act as both neutral (LH) and monoanionic (L^-) chelates suitable for transition-metal chemistry,

[a] *I. Koehne, Dr. S. Bachmann, Dr. T. Niklas, Dr. R. Herbst-Irmer, Prof. Dr. D. Stalke*
Universität Göttingen
Institut für Anorganische Chemie
Tammannstraße 4, 37077 Göttingen (Germany)
E-mail: dstalke@chemie.uni-goettingen.de
Homepage: www.uni-goettingen.de/de/53448.html

[**] *NacNac = β-diketiminate.*

Supporting information and the ORCID number(s) for the author(s) of this article can be found under https://doi.org/10.1002/chem.201702378.

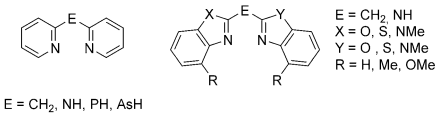

Scheme 2. NacNac related bis(heterocyclo)methane, -amine, -phosphane, and -arsine ligand systems.

they have attracted little attention in coordination chemistry so far.[34,35]

Nevertheless, our group showed that bis(benzoxazol-2-yl)- and bis(benzothiazol-2-yl)methanides are versatile platforms for Group 1 and 13 metal complexes.[36,37] This chemistry was extended to the corresponding N-bridged derivatives[38] and, most recently, to benzimidazol- and asymmetrically substituted bis(heterocyclo)methane species (Scheme 2, right).[39] All the abovementioned methanide or amide ligand systems with H, Me, or OMe substituents at the C4 position only display limited steric demand in close proximity to the coordination pocket. Herein, we present our successful effort to introduce bulky *t*Bu substituents to a bis(benzoxazol-2-yl)methane system to supply enhanced steric shielding and enable s-block metal-ion coordination.

Results and Discussion

To obtain a bis(benzoxazol-2-yl)methane derivative that provides analogous steric demand to the NacNac five-membered coordination ring, a synthetic route to the corresponding 2-aminophenol derivative had to be established; with the 2-aminophenol derivative in hand, the desired ligand species should be easily accessible through a double cyclocondensation reaction with a suitable C_3-linker unit according to literature procedures.[37,40] With this in mind, and to cope with the unselective nature of the common nitration reaction of aromatic compounds with nitric acid, the synthetic protocol commenced from symmetrically substituted 3,5-di-*tert*-butylphenol, which features two equivalent *ortho* positions and a sterically hindered *para* position. Addition of nitric acid (1 equiv) to the starting material gave the corresponding mono-*ortho*-substituted derivative 3,5-di-*tert*-butyl-2-nitrophenol (**1**) in an appreciable yield of 45% (Scheme 3, top).[1] The IR spectrum of **1** shows characteristic vibrational bands for the symmetric ($\tilde{\nu}$ = 1366 cm^{-1}) and asymmetric ($\tilde{\nu}$ = 1518 cm^{-1}) NO_2 stretch. Subsequent hydration of pure **1** with H_2 (1.5 bar) and a heterogeneous hydration catalyst (Pd/C) gave 3,5-di-*tert*-butyl-2-aminophenol (**2**) in an excellent yield (90%) within 24 h. Again, the IR spectrum of **2** showed characteristic vibrational bands for the symmetric ($\tilde{\nu}$ = 3316 cm^{-1}) and asymmetric ($\tilde{\nu}$ = 3415 cm^{-1}) NH_2 stretch. Compound **2** (2 equiv) was reacted with the C_3 linker ethyl-bisimidate dihydrochloride (1 equiv), whereupon a double cyclocondensation afforded the desired ligand bis(4,6-*t*Bu-benzoxazol-2-yl)methane (**3**) in sufficient yield (18–21%, Scheme 3, bottom).

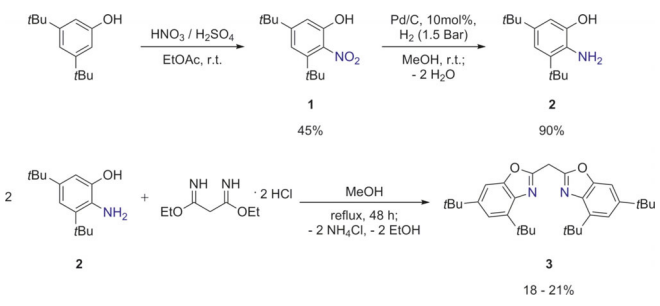

Scheme 3. Synthesis of the aminophenol derivative **2** (top) and bis(4,6-*t*Bu-benzoxazol-2-yl)methane (**3**) (bottom).

Compound **3** crystallizes in the monoclinic space group $P2_1/n$ and contains one molecule in the asymmetric unit (Figure 1). The whole molecule shows positional disorder about two positions. Some general trends among the related bis(benzoxazol-2-yl)methane derivatives $(NCOC_6H_4)_2CH_2$ (**I**)[36] and $(4\text{-}MeNCOC_6H_3)_2CH_2$ (**II**)[37] are discussed below (Table 1).

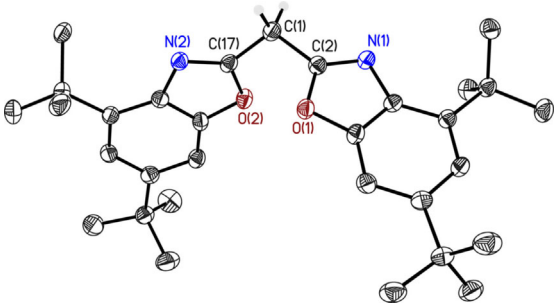

Figure 1. Molecular structure of **3**. Anisotropic displacement parameters are depicted at the 50% probability level. Hydrogen atoms are omitted for clarity, except for those at the bridging methylene position. See Tables 1 and 4 for structural data.

Table 1. Selected angles [°] and average bond lengths [Å] for **I**, **II**, and **3**.

Compound	C_{ipso}–C(1)	C_{ipso}–N	C_{ipso}-C(1)-C_{ipso}
I	1.489(2)	1.286(2)	120.2(3)
II	1.487(2)	1.291(2)	110.8(1)
3	1.495(2)	1.289(2)	111.2(1)

In all three compounds the corresponding averaged C_{ipso}–C(1) and C_{ipso}–N bond lengths are within the same range and show no significant deviation as the steric demand of the substituents increases. However, the C_{ipso}-C(1)-C_{ipso} angle is significantly narrowed from 120.2(3)° in unsubstituted **I** to 110.8(1)° in 4-methyl-substituted compound **II**. This strong deviation might also be caused by the formation of a 3D network of C–H···N hydrogen bonds in the solid state of **II**. In 4,6-*tert*-butyl-substituted compound **3** the parent C_{ipso}-C(1)-C_{ipso} angle is slightly increased to 111.2(1)°. The two benzoxazole moieties in **I**, **II**, and **3** display a twisted orientation due to the distorted tetrahedral coordination around the bridging C(1) atom. In **I** and **II** one heterocycle stays almost in plane with the C_3-linker unit, whereas the other shows almost perpendicular torsion with respect to the linker. In contrast, **3** shows a notably stronger twisted orientation due to its greater steric requirements.

In **3** both N-C_{ipso}-C(1)-C_{ipso} torsion angles display similar torsion out of the C_3-linker unit plane (average = 131.6°). Notably, the coordination pocket in **I** and **II** in the solid state comprises the C_{ipso}-C(1)-C_{ipso} bridging moiety and the ring nitrogen atoms, whereas in **3** the oxygen atoms are twisted inwards and occupy the position of the donor atoms, which minimizes steric repulsion between the neighboring *t*Bu groups.

When **3** was treated overnight with *t*BuLi at −50 °C the precursor complex **4** was obtained in good yield (74%, Scheme 4).

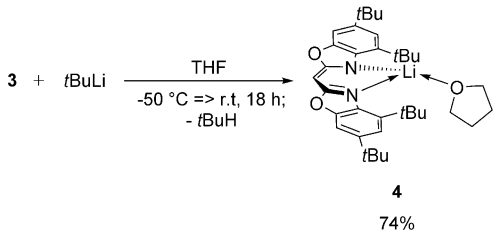

4

74%

Scheme 4. Synthesis of [Li{(4,6-*t*Bu-NCOC$_6$H$_2$)$_2$CH}THF] (**4**).

Lithium species **4** crystallizes in the monoclinic space group *C*2/*c* and contains one molecule in the asymmetric unit. (Figure 2 and Table 2). The central lithium cation adopts trigonal pyramidal geometry from coordination by two ring nitrogen atoms of the parent monoanionic methanide ligand and one oxygen atom of a THF molecule. The hard metal coordinates with the nitrogen atoms despite the steric strain provided by the cross-ligand *t*Bu substituents. Additionally, lithium is lifted 0.629(6) Å from the plane defined by N(1)-O(3)-N(2). Interestingly, the fourth coordination site at the Li^+ ion is shielded by the 4-*t*Bu substituents of the ligand periphery, which prevents it from being tetrahedrally coordinated by inclusion of a second THF donor base. Furthermore, the steric repulsion of the *t*Bu substituents forces the lithium cation 0.696(7) Å out of the plan of the chelating C_3N_2 ring. To the best of our knowledge **4** is the first NacNac-related bis(benzoxazol-2-yl)-methanide–lithium complex that displays trigonal pyramidal coordination and is reminiscent of the related three-coordinate trigonal planar lithium complexes [Li(L)(Dipp$_2$NacNac][8] (L = Et_2O or THF). The reported averaged Li–N bond lengths of these complexes [1.915(4) (L = Et_2O) and 1.958(5) Å (L = THF)] are in good agreement with the average distance in **4** (1.951(6) Å), which most closely matches the THF-solvated complex. The same is true for the corresponding N-Li-N bite angles, though in this case the value of the Et_2O-solvated complex (99.9(2)°) is most similar to **4** (99.0(3)°). The values for the C_{ipso}-C(1)-C_{ipso} angle in the ligand periphery of the NacNac complexes are very similar (129.5(2)° and 128.6(3)°), whereas in **4** this angle experiences a considerable reduction to 121.7(3)°. Just like in **4**, the lithium cation in the related complex [Li(Dipp$_2^{Ph}$NacNac)(Et_2O)],[41] which bears phenyl rather than methyl groups on the ligand backbone, is also reported to show a slight dislocation of the metal ion from the plane of the ligand framework. Nevertheless, the metal ion was still considered to be in a trigonal planar geometry. Furthermore, even the related four-coordinate bis(pyridyl)methanide complex [Li{(2-NC$_5$H$_4$)$_2$CH}(THF)$_2$][26] and its higher homologue the bis(pyridyl)phosphide complex [Li{(2-NC$_5$H$_4$)$_2$P}(THF)$_2$][24] show comparable structural features to **4**.

Reaction of the parent ligand system **3** with potassium hydride in THF gives the corresponding polymeric precursor **5** in excellent yield (80%, Scheme 5). Complex **5** crystallizes in the

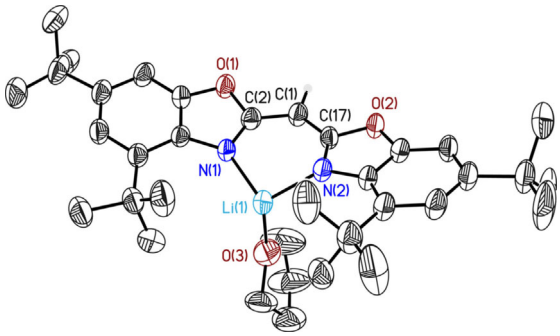

Figure 2. Molecular structure of **4**. Anisotropic displacement parameters are depicted at the 50% probability level. Hydrogen atoms are omitted for clarity, except for that at the bridging methylene position. See Tables 2 and 4 for structural data.

Table 2. Selected average bond lengths [Å] and angles [°] for **4**–**6**.				
Compound	N–M	N-M-N	C_{ipso}-C(1)-C_{ipso}	M–C_3N_2 plane distance
4	1.951(6)	99.0(3)	121.7(3)	0.696(7)
5	–	65.99(2)	125.5(6)	2.311(7)
6	2.1786(2), 2.1602(2)	99.83(6)	128.9(2)	0.010(2)

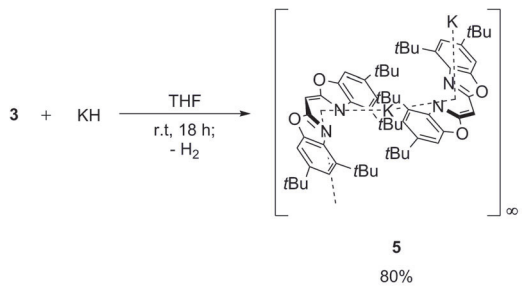

5

80%

Scheme 5. Synthesis of [K{η^5-(4,6-*t*Bu-NCOC$_6$H$_2$)$_2$CH}]$_\infty$ (**5**).

triclinic space group $P\bar{1}$. The asymmetric unit contains one ligand molecule and two potassium cations, which both lie on an inversion center (see the Supporting Information). The bond lengths and angles determined for this structure suffer from a certain unreliability due to the formation of small acicular crystals with decreased scattering abilities, which cause low data resolution. Hence, no detailed discussion of these parameters is attempted. Only the unambiguous data for the N-M-N bite angle and the dislocation of the potassium cation from the chelating C_3N_2 plane are discussed below.

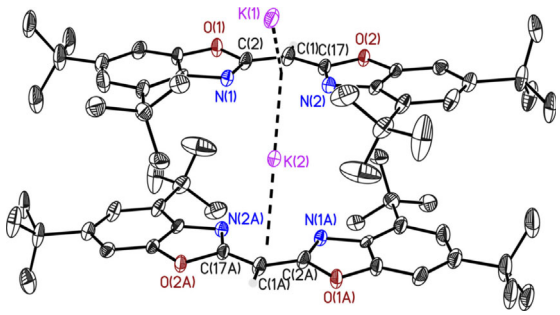

Figure 3. Excerpt from the molecular structure of **5**, which forms infinite linear coordination-polymer strands. Anisotropic displacement parameters are depicted at the 50% probability level. Hydrogen atoms are omitted for clarity, except for those at the bridging methylene positions. See Tables 2 and 4 for structural data.

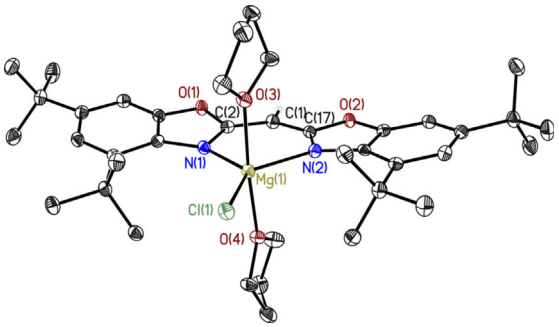

Figure 4. Molecular structure of **6**. Anisotropic displacement parameters are depicted at the 50% probability level. The co-crystalized pentane molecule and hydrogen atoms, except for that at the bridging methylene position, are omitted for clarity. See Tables 2 and 4 for structural data.

The central potassium cation is sandwiched by η^5 coordination to two C_3N_2 planes, which forms infinite linear strands (Figure 3). Again, the steric demand of the *t*Bu substituents inhibits coordination of THF donor molecules to the metal ion. Relative to the structures of **4** and **6** the N-M-N bite angle in **5** is strongly reduced to realize the favored η^5 coordination of the soft potassium ion to the soft, undirected π density of the deprotonated ligand molecules.[42,43] Nevertheless, the average dislocation of the metal ions from the C_3N_2 plane (2.311(7) Å) and the average N-M-N bite angle (65.99(2)°) are in good agreement with the values found for a related dimeric NacNac-derived complex with an average C_3N_2 plane distance of 2.29(1) Å and mean bite angle of 65.7(2)°.[44] In contrast, the dislocation found in **5** falls at the short end of the range for other non-NacNac related compounds that display potassium–π-system interactions. For example, the η^6- and η^5-bound species $[K(PhCH_2)(PMDETA)]_\infty$[45] and $[K(C_5Me_5)\cdot 2\,Py]_\infty$[46] (PMDETA = $(Me_2NCH_2CH_2)_2NMe$), Py = pyridyl) also adopt a polymeric structure in the solid state but have significantly longer potassium–π-plane distances (3.150(2) and 2.79(1) Å, respectively).

When **3** (1 equiv) was suspended with the Hauser-type base $(iPr)_2NMgCl$ (2 equiv) the corresponding heteroleptic magnesium chloride complex **6** was obtained in a moderate yield (48%) within 18 h (Scheme 6). Complex **6** crystallizes in the monoclinic space group $P2_1/n$. It contains one molecule and a co-crystallized pentane molecule in the asymmetric unit. An Addison parameter[47] of 0.74 undoubtedly indicates a five-coordinate trigonal bipyramidal coordination around the central magnesium ion by two chelating ring nitrogen atoms and a chloride ligand forming the equatorial plane and two THF donor molecules at the apical positions (Figure 4). The Mg^{2+} cation shows an in-planar arrangement to the chelating C_3N_2 moiety (a dislocation of only 0.010(2) Å) and fits perfectly into the provided coordination pocket. The N-M-N bite angle is not significantly changed relative to **4**, whereas the corresponding N–M bond lengths and C_{ipso}-C(1)-C_{ipso} angle are increased relative to **4** (2.1786(2) and 2.1602(2) Å vs 1.951(6) Å; 128.9(2)° vs 121.7(3)°), which is in good agreement with the elevated ionic radius of the Mg^{2+} cation. Complex **6** is the first example of a NacNac-related bis(benzoxazol-2-yl)methanide magnesium complex with a trigonal bipyramidal geometry. Comparable trigonal bipyramidal NacNac-based magnesium complexes, such as the dinuclear $[Mg_2(\{N(SiMe_3)C(tBu)C(H)\}_2\{2,3\text{-}C_4H_2N_2\})Br_2(THF)_4]$[44] and the tripodal species $[(\{\kappa^3\text{-}N,N',O\text{-}(DippNCMe)_2(OCCPh_2)CH\}Mg\{\mu\text{-}I\})_2]$ and $[(\{\kappa^3\text{-}N,N',O\text{-}(DepNCMe)_2(OCCPh_2)CH\}Mg)_2(\mu\text{-}\kappa^2\text{:}\kappa^2\text{-}S_2O_4)]$ (Dep = 2,6-diethylphenyl),[22] exhibit values from 2.155–2.132 Å, thus have slightly shorter Mg–N bonds than in **6**. Interestingly, in the six-coordinate complex $[Mg\{(pz^*)_3C\}_2]$ (pz^* = 3,5-dimethylpyrazolyl), the Mg–N bond length is only slightly longer (2.197 Å) than in **6**.[48]

Reduction of **6** was attempted to synthesize a potentially dimeric, low-oxidation-state Mg^I–Mg^I complex. Unfortunately, reactions with potassium metal or potassium graphite as the reducing agent at room temperature or 0 °C gave the homoleptic Mg^{2+} complex **7** in good yield (76–80%, Scheme 7). The

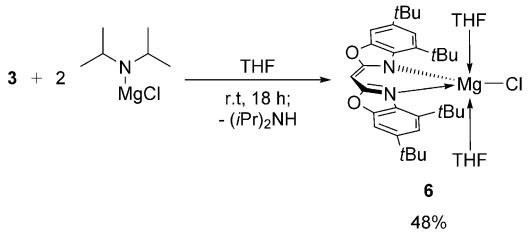

Scheme 6. Synthesis of $[MgCl\{(4,6\text{-}tBu\text{-}NCOC_6H_2)_2CH\}(THF)_2]$ (**6**).

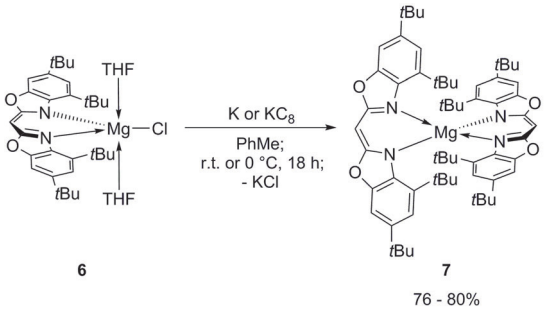

Scheme 7. Synthesis of $[Mg\{(4,6\text{-}tBu\text{-}NCOC_6H_2)_2CH\}_2]$ (**7**).

formation of complex **7** could be the result of a Schlenk equilibrium redistribution of a heteroleptic complex towards its homoleptic equivalent or a transient Mg^{+} complex that is prone to disproportionation to Mg^{0} and Mg^{2+} and the resulting excess of negatively charged ligand molecules. Similar observations were made by Bonyhady et al. during their attempts to reduce the related NacNac precursor complex [MgI(^{Ph}NacNac)(Et_2O)] with sodium or potassium metal.[21] Because of the high solubility of **7** no single crystals suitable for X-ray diffraction experiments have been obtained as yet. Nevertheless, formation of the homoleptic compound **7** was confirmed by LIFDI MS (liquid-injection field-desorption ionization mass spectrometry), which undoubtedly displayed the isotopic pattern and the mass of an Mg^{2+} ion chelated by two ligand molecules.

The presence of N- and O-donor sites within the deprotonated bis(4,6-*t*Bu-benzoxazol-2-yl)methanide ligand **3** means that two symmetrical coordination modes are feasible: an exclusively N-bound (**7**) and a solely O-bound species (**7a**) (Figure 5).

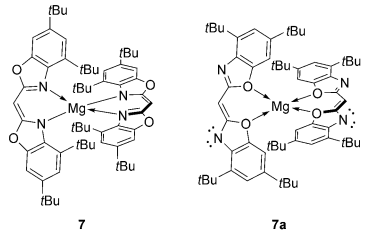

Figure 5. Comparison of N-bound (**7**) and O-bound (**7a**) coordination modes.

Due to the presence of only one set of signals in the ^{1}H NMR spectrum of **7** a third feasible coordination motif comprising one N- and one O-bound ligand can be directly ruled out. From a coordination chemistry point of view a solely N-bound complex should be less favored due to the steric crowding caused by the C(4)–*t*Bu groups occupying space around the Mg^{2+} ion. Hence, advanced NMR techniques were applied to determine the correct coordination mode.

First, the N-binding motif of deprotonated **3** to the Mg^{2+} ion in solution was evaluated by using the δ_N value determined from a ^{15}N-^{1}H HMBC experiment. The resonance at $\delta_N = -213$ ppm is close to the shift that **6** exhibits ($\delta_N = -217$ ppm) in the N-binding mode, which was confirmed by single-crystal X-ray diffraction. This motif is further corroborated by NOESY experiments. The cross-peak between the C(4)–*t*Bu substituents and the methylene bridging moiety of the second ligand molecule is much stronger than between the C(6)–*t*Bu groups and that bridging motif (Figure 6). The correlated spatial proximity can only be rationalized by the N-binding mode of **7** (see the structural models in the Supporting Information). Additionally, we conducted a preliminary study which showed that one-bond residual dipolar couplings (RDCs) between carbon and hydrogen atoms can also be employed to solve this stereochemical problem (see the Supporting Information).

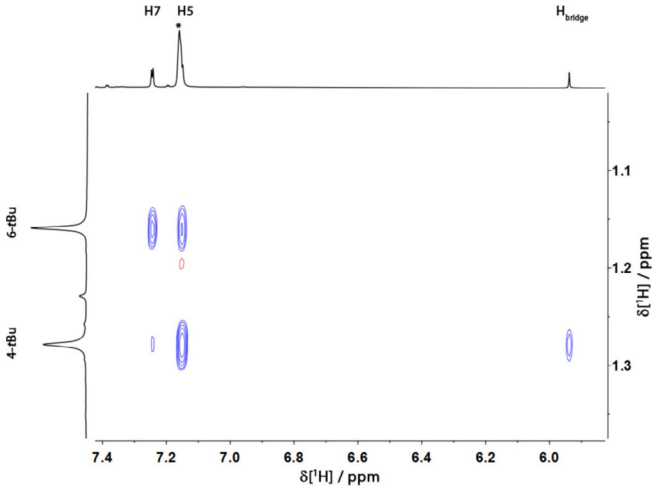

Figure 6. Excerpt from the ^{1}H-NOESY spectrum of **7** in C_6D_6 (*). For clarity, only the relevant cross-peaks are shown.

DOSY investigations

The results of the ^{1}H-DOSY external calibration curve (ECC) molecular weight (*MW*) estimation[49–51] used to clarify the structures of **4**–**7** in solution are discussed in detail below. Previous studies showed that for most organometallic compounds the dissipated spheres and ellipsoids (DSE) calibration curve is the most suitable for an accurate estimation.[52] Therefore, only values from the DSE and, for comparison, from the merge calibration curve are considered (Table 3). The *MW* of **4** in solution was estimated to be 575 (DSE) and 643 g mol^{-1} (merge). Within the error range these values either fit a three- (553 g mol^{-1}) or four-coordinate (625 g mol^{-1}) species with one or two attached THF molecules, respectively, which indicates the presence of a dynamic exchange process. Compared with the ^{1}H NMR spectrum of **4**, which shows one THF molecule attached to the complex, it is most likely that the three-coordinate structure observed in the solid state is retained in solution. Furthermore, superimposition of the ^{1}H- and ^{7}Li-DOSY experiments for **4** shows that all complex-related signals have

Table 3. ^{1}H-DOSY ECC *MW* estimation of **4**–**7** in C_6D_6 at r.t.

Aggregate	*x*	MW_{theo}[a] [g mol−1]	MW_{DSE} [g mol−1] (MW_{dif}[b] [%])	MW_{merge} [g mol−1] (MW_{dif} [%])
[Li(*t*BuBox)(THF)$_x$][c] (**4**)	0	481	575 (−16)	643 (25)
	1	553	575 (−4)	643 (−14)
	2	625	575 (9)	643 (−3)
[K(*t*BuBox)(C_6H_6)$_x$] (**5**)	0	513	490 (−8)	620 (−17)
	1	591	490 (6)	620 (−5)
	2	669	490 (20)	620 (8)
[MgCl(*t*BuBox)(THF)$_x$] (**6**)	0	533	609 (−12)	685 (−22)
	1	606	609 (0)	685 (−12)
	2	678	609 (11)	685 (−1)
[Mg(*t*BuBox)$_2$] (**7**)	–	972	857 (14)	993 (−2)

[a] MW_{theo} = Theoretical *MW*. [b] Percentage difference between the theoretical and calculated *MW* value. [c] *t*BuBox = bis(4,6-*t*Bu-benzoxazol-2-yl)-methanide.

one diffusion coefficient, which indicates the presence of a strong contact ion pair (see the Supporting Information).

The *MW* of potassium complex **5** was estimated to be 490 (DSE) and 620 g mol^{-1} (merge), which excludes retention of the polymeric structure in solution. More likely, monomeric structures are formed with one additional benzene molecule to satisfy the coordination sphere of the cation; a theoretical *MW* of 591 g mol^{-1} calculated for this scenario provided the best fit to the data.

The *MW* of magnesium complex **6** in solution was estimated to be 609 (DSE) and 685 g mol^{-1} (merge), which fits to a four- or five-coordinate species with one or two attached THF molecules, respectively. Again, these findings show that the THF ligands are subject to rapid dynamic exchange processes, which exacerbates a reliable conclusion about the molecular shape of **6** in solution. The *MW* of the homoleptic magnesium complex **7** in solution was estimated to be 857 (DSE) and 993 g mol^{-1} (merge). The latter estimation, in particular, is in good agreement with the theoretical *MW* of 972 g mol^{-1} for **7**, and also supports the LIFDI MS results.

Conclusion

The family of bis(benzoxazol-2-yl)methane ligands was extended by introducing the new bulky bis(4,6-*t*Bu-benzoxazol-2-yl)-methane ligand **3**. Concerted deprotonation–metalation reactions were carried out on **3** with typical alkali-metal reagents such as *t*BuLi or KH, and the corresponding precursor complexes **4** and **5** were formed. Furthermore, reaction of **3** with the Hauser-type base (*i*Pr)$_2$NMgCl yielded trigonal bipyramidal magnesium chloride species **6**. All of the compounds show interesting structural features in the solid state and in solution, studied by single-crystal X-ray diffraction and DOSY NMR spectroscopy, respectively. Attempts to obtain a low-oxidation-state, potentially dimeric Mg^{I}–Mg^{I} species by reduction of **6** with potassium metal or KC_8 afforded the homoleptic Mg^{2+} complex **7**, which was assumed to form by disproportionation or a Schlenk equilibrium type redistribution. Despite the lack of X-ray data for **7**, its structure was successfully determined by advanced NMR spectroscopic techniques (NOESY, clean-in-phase HSQC, and DOSY) and LIFDI MS. Our efforts to expand the class of sterically demanding, heteroaromatic-substituted methanides that mimic the ubiquitous NacNac ligand system and their application as platforms for the metal-mediated activation of small molecules are ongoing.

Experimental Section

Procedures

All manipulations were carried out under an inert argon atmosphere by using Schlenk techniques[53] or in an argon drybox. All solvents used for the metalation reactions were distilled from Na or K before use. Starting materials were purchased commercially and were used as received, unless stated otherwise. (*i*Pr)$_2$NMgCl and KC_8 were synthesized according to literature procedures.[54,55] ^{1}H- and ^{13}C NMR spectra were recorded with a Bruker Avance 300 or 400 MHz spectrometer and are referenced to the residual proton signal of the deuterated solvent.[56] Deuterated solvents were dried over activated molecular sieves (3 Å) then stored in an argon drybox. Elemental analyses (CHN) were carried out with a Vario EL3 instrument at the Mikroanalytisches Labor, Institut für Anorganische Chemie, University of Göttingen. All LIFDI MS spectra were performed with a Jeol AccuTOF spectrometer. NOESY spectra were recorded with a Bruker Avance III 400 MHz instrument with a relaxation delay of 1.5 s and 0.5 s mixing time. 2048×512 data points were sampled over a spectral width of $\delta = 12$ ppm (number of scans = 4). HMBC spectra were recorded with a Bruker Avance III 400 MHz instrument by using a relaxation delay of 2 s. 2048×256 data points were sampled over a spectral width of $\delta = 12$ ppm in F2 and $\delta = 200$ ppm in F1 (number of scans = 2).

Synthesis

3,5-Di-*tert*-butyl-2-nitrophenol (1): 3,5-Di-*tert*-butyl-phenol (10.0 g, 48.5 mmol, 1.00 equiv) was dissolved in ethyl acetate (800 mL). Under vigorous stirring, nitric acid (1:2 HNO_3/H_2SO_4, 9.32 mL, 48.5 mmol, 1.00 equiv) was slowly added portionwise (0.20 mL min^{-1}). After complete addition, the mixture was stirred for an additional 15 minutes then transferred to a separation funnel. The organic phase was washed with H_2O and brine until an almost neutral pH of the aqueous phase was achieved. The organic phase was separated, dried over anhydrous $MgSO_4$, and the solvent was removed under reduced pressure. The reddish-orange residue was recrystallized several times from pentane to give **1** (5.44 g, 45%) as a yellow solid. ^{1}H NMR (300 MHz, [D$_6$]acetone, 25 °C): $\delta = 9.12$ (s, 1H; OH), 7.12 (d, ^4J(H,H) = 1.9 Hz, 1H; H4), 7.01 (d, ^4J(H,H) = 1.9 Hz, 1H; H6), 1.37 (s, 9H; 3-C(C*H*$_3$)$_3$), 1.30 ppm (s, 9H; 5-C(C*H*$_3$)$_3$); ^{13}C NMR (75 MHz, [D$_6$]acetone, 25 °C): $\delta = 154.3$ (1C; C5), 149.6 (1C; C1), 141.7 (1C; C3), 138.9 (1C; C2), 116.6 (1C; C4), 112.8 (1C, C6), 36.6 (1C; 3-*C*(CH$_3$)$_3$), 35.8 (1C; 5-*C*(CH$_3$)$_3$), 31.5 (1C; 3-C(*C*H$_3$)$_3$), 31.2 ppm (1C; 5-C(*C*H$_3$)$_3$); IR (ATR): $\tilde{\nu} = 3423$, 2956, 2908, 2872, 1592, 1518 (NO_2 asymmetric stretch (as.)), 1366 (NO_2 symmetric stretch (s.)), 1291, 978, 860, 666 cm^{-1}; MS (EI, 70 eV): *m/z* (%): 251.3 (30) [*M*$^+$], 236.2 (100) [*M*−OH+H$^+$]; elemental analysis calcd (%) for $C_{14}H_{21}NO_3$: C 66.91, H 8.42, N 5.57; found: C 65.67, H 8.37, N 5.39.

3,5-Di-*tert*-butyl-2-aminophenol (2): In a 100 mL pressure flask with screw cap and Young valve, **1** (4.00 g, 15.9 mmol, 1.00 equiv) was dissolved in MeOH (20 mL) and Pd/C (10%, 180 mg, 1.59 mmol, 0.10 equiv) was added under cooling with a liquid N_2 bath. The resulting suspension was degassed via three freeze–pump–thaw cycles, and then a H_2 atmosphere (1.5 bar) was established above the frozen suspension and the mixture was stirred at RT for 24 h. All solid material was removed by filtration via cannula under an argon atmosphere and then the filtrate was evaporated under reduced pressure. The crude product was purified by recrystallization from $CHCl_3$ to give **2** (3.17 g, 90%) as a white fluffy solid. ^{1}H NMR (300 MHz, [D$_6$]acetone, 25 °C): $\delta = 7.86$ (s, 1H; OH), 6.81 (d, ^4J(H,H) = 2.2 Hz, 1H; H4), 6.74 (d, ^4J(H,H) = 2.2 Hz, 1H; H6), 4.02 (s, 2H; NH_2), 1.41 (s, 9H; 3-C(C*H*$_3$)$_3$), 1.22 ppm (s, 9H; 5-C(C*H*$_3$)$_3$); ^{13}C NMR (75 MHz, [D$_6$]acetone, 25 °C): $\delta = 152.9$ (1C; C5), 145.2 (1C; C1), 135.4 (1C; C3), 133.4 (1C; C2), 114.8 (1C; C4), 104.5 (1C; C6), 35.3 (1C; 3-*C*(CH$_3$)$_3$), 35.2 (1C; 5-*C*(CH$_3$)$_3$), 32.2 (1C; 3-C(CH$_3$)$_3$), 30.0 ppm (1C; 5-C(*C*H$_3$)$_3$); IR (ATR): $\tilde{\nu} = 3415$ (NH_2 as.), 3316 (NH_2 s.), 2954, 1580, 1418, 1301, 1171, 957, 860, 789 cm^{-1}; MS (EI, 70 eV): *m/z* (%): 221.3 (25) [*M*$^+$], 206.3 (100) [*M*–NH_2^+]; elemental analysis calcd (%) for $C_{14}H_{23}NO$: C 75.97, H 10.47, N 6.33; found: C 74.08, H 10.12, N 6.14.

(4,6-*t*Bu-NCOC$_6$H$_2$)$_2$CH$_2$ (3): Compound **2** (8.00 g, 36.1 mmol, 2.00 equiv) and ethylbisimidate dihydrochloride (4.17 g, 18.1 mmol,

1.00 equiv) were dissolved in MeOH (60 mL) and heated at 85 °C for 48 h. The mixture was cooled to RT and the solvent was removed under reduced pressure. The residue was extracted with pentane (3×30 mL) with the help of a supersonic bath, and then filtered. The filtrate was evaporated under reduced pressure and the crude product was recrystallized from EtOH to give **3** as a white crystalline solid (1.55–1.80 g, 18–21%). ^{1}H NMR (300 MHz, $CDCl_3$, 25 °C): δ = 7.35 (d, ^4J(H,H) = 1.7 Hz, 2H; H5), 7.28 (d, ^4J(H,H) = 1.7 Hz, 2H; H7), 4.61 (s, 2H; CH_2), 1.55 (s, 18H; 4-C(CH_3)$_3$), 1.36 ppm (s, 18H; 6-C(CH_3)$_3$); ^{1}H NMR (300 MHz, C_6D_6, 25 °C): δ = 7.40 (d, ^4J(H,H) = 1.7 Hz, 2H; H5), 7.21 (d, ^4J(H,H) = 1.7 Hz, 2H; H7), 4.20 (s, 2H; CH_2), 1.68 (s, 18H; 4-C(CH_3)$_3$), 1.23 ppm (s, 18H; 6-C(CH_3)$_3$); ^{1}H NMR (300 MHz, [D$_8$]THF, 25 °C): δ = 7.42 (d, ^4J(H,H) = 1.7 Hz, 2H; H5), 7.30 (d, ^4J(H,H) = 1.7 Hz, 2H; H7), 4.66 (s, 2H; CH_2), 1.54 (s, 18H; 4-C(CH_3)$_3$), 1.35 ppm (s, 18H; 6-C(CH_3)$_3$); ^{13}C NMR (75 MHz, $CDCl_3$, 25 °C): δ = 157.7 (2C; C1), 152.0 (2C; C8), 148.5 (2C; C6), 142.6 (2C; C4), 137.2 (2C; C3), 118.2 (2C; C5), 105.2 (2C; C7), 35.6 (2C; 4-*C*(CH_3)$_3$), 35.4 (2C; 6-*C*(CH_3)$_3$), 31.9 (2C; 6-C(CH_3)$_3$), 30.5 (2C; 4-C(CH_3)$_3$), 29.8 ppm (1C, C_{bridge}); ^{13}C NMR (75 MHz, C_6D_6, 25 °C): δ = 158.3 (2C; C1), 152.6 (2C; C8), 148.6 (2C; C6), 142.9 (2C; C4), 137.8 (2C; C3), 118.2 (2C; C5), 105.6 (2C; C7), 35.9 (2C; 4-*C*(CH_3)$_3$), 35.3 (2C; 6-*C*(CH_3)$_3$), 31.8 (2C; 6-C(CH_3)$_3$), 30.6 (2C; 4-C(CH_3)$_3$), 29.5 ppm (1C; C_{bridge}); IR (ATR): $\tilde{\nu}$ = 2956, 1601 (C=N), 1396, 1243, 1153, 993, 853, 777 cm^{-1}; MS (EI, 70 eV): *m/z* (%): 474.3 (40) [M^+], 459.3 (100) [$M-CH_3^+$]; elemental analysis calcd (%) for $C_{31}H_{42}N_2O_2$: C 78.44, H 8.92, N 5.90; found: C 77.45, H 8.55, N 5.84.

[Li{(4,6-*t*Bu-NCOC$_6$H$_2$)$_2$CH}THF] (4): Compound **3** (300 mg, 632 μmol, 1.00 equiv) was dissolved in THF (15 mL) and cooled to −50 °C. Under stirring, *t*BuLi (2.05 M in hexane, 0.32 mL, 656 μmol, 1.04 equiv) was slowly added dropwise. After complete addition the mixture was stirred at −50 °C for an additional 15 min. The cooling bath was removed and the solution was stirred at RT for 5 h. The solvent was removed under reduced pressure then the residue was washed with ice cold pentane (3×10 mL), filtered via cannula, and dried under reduced pressure to give **4** (259 mg, 74%) as a pale-yellow solid. Crystals suitable for X-ray diffraction were obtained from a saturated solution in hexane at rt. ^{1}H NMR (300 MHz, C_6D_6, 25 °C): δ = 7.34 (d, ^4J(H,H) = 1.8 Hz, 2H; H7), 7.30 (d, ^4J(H,H) = 1.8 Hz, 2H; H5), 5.60 (s, 1H; H_{bridge}), 3.15 (m, 4H; OCH_2CH$_2$), 1.58 (s, 18H; 4-C(CH_3)$_3$), 1.34 (s, 18H; 6-C(CH_3)$_3$), 0.93 ppm (m, 4H; OCH$_2$$CH_2$); ^{13}C NMR (75 MHz, C_6D_6, 25 °C): δ = 169.9 (2C; C1), 150.8 (2C; C8), 143.1 (2C; C6), 139.0 (2C; C4), 134.1 (2C; C3), 117.5 (2C; C5), 104.4 (2C; C7), 68.6 (2C; OCH$_2$CH$_2$), 57.3 (1C; C_{bridge}), 35.1 (2C; 6-*C*(CH_3)$_3$), 35.0 (2C; 4-*C*(CH_3)$_3$), 32.1 (6C; 6-C(CH_3)$_3$), 31.1 (6C; 4-C(CH_3)$_3$), 25.1 ppm (2C; OCH$_2$$CH_2$); ^{7}Li NMR (116 MHz, C_6D_6, 25 °C): δ = 2.76 ppm (s); MS (LIFDI): *m/z* (%): 480.2 (20) [M−THF], 474.3 (100) [4,6-tBu-NCOC$_6$H$_2$)$_2$CH$_2$]; elemental analysis calcd (%) for $C_{35}H_{49}LiN_2O_3$: C 76.06, H 8.94, N 5.07; found: C 75.18, H 8.86, N 5.36.

[K{η^5-(4,6-*t*Bu-NCOC$_6$H$_2$)$_2$CH}]$_\infty$ (5): KH (33.0 mg, 696 μmol, 1.10 equiv) was suspended in THF (10 mL) and **3** (300 mg, 633 μmol, 1.00 equiv) in THF (5 mL) was added dropwise via syringe. The mixture was stirred at RT for 18 h. The suspension was filtered via cannula, and the filtrate was evaporated under reduced pressure. The residue was washed with pentane (3×10 mL), filtered, and dried under reduced pressure to give **5** as a white solid (296 mg, 80%). Recrystallization by evaporation of pentane into a saturated solution of **5** in THF at RT gave colorless needle-shaped crystals. ^{1}H NMR (300 MHz, [D$_8$]THF, 25 °C): δ = 7.01 (d, ^4J(H,H) = 1.7 Hz, 2H; H7), 6.97 (d, ^4J(H,H) = 1.8 Hz, 2H; H5), 4.56 (s, 1H; H_{bridge}), 1.54 (s, 18H; 4-C(CH_3)$_3$), 1.32 ppm (s, 18H; 6-C(CH_3)$_3$); ^{13}C NMR (75 MHz, [D$_8$]THF, 25 °C): δ = 169.0 (2C; C1), 151.2 (2C; C8), 142.7 (2C; C6), 141.3 (2C; C4), 135.4 (2C; C3), 116.1 (2C; C5), 103.2 (2C; C7), 55.3 (1C; C_{bridge}), 35.9 (2C; 6-*C*(CH_3)$_3$), 35.5 (2C; 4-*C*(CH_3)$_3$), 32.6 (6C; 6-C(CH_3)$_3$), 30.9 ppm (6C; 4-C(CH_3)$_3$); MS (LIFDI): *m/z* (%): 551.1 (33) [M−THF+K^+], 512.2 (100) [M−THF], 474.2 (42) [4,6-*t*Bu-NCOC$_6$H$_2$)$_2$CH$_2$]; elemental analysis calcd (%) for $C_{31}H_{41}KN_2O_2$: C 72.61, H 8.06, N 5.46; found: C 70.34, H 8.12, N 5.25.

[MgCl{(4,6-*t*Bu-NCOC$_6$H$_2$)$_2$CH}(THF)$_2$] (6): Compound **3** (300 mg, 633 μmol, 1.00 equiv) and (*i*Pr$_2$N)MgCl·(THF)$_{0.65}$ (283 mg, 1.39 mmol, 2.20 equiv) were suspended in THF (15 mL) and stirred at RT for 18 h. The solvent was removed under reduced pressure and the residue was extracted with pentane (3×10 mL) then filtered via cannula. The filtrate was concentrated to two thirds of its original volume then stored at −28 °C to afford **6** (228 mg, 48%) as colorless plate-shaped crystals suitable for X-ray diffraction. ^{1}H NMR (300 MHz, C_6D_6, 25 °C): δ = 7.42 (d, ^4J(H,H) = 2.0 Hz, 2H; H7), 7.28 (d, ^4J(H,H) = 2.0 Hz, 2H; H5), 5.62 (s, 1H; H_{bridge}), 3.57 (m, 8H; OCH_2CH$_2$), 1.84 (s, 18H; 4-C(CH_3)$_3$), 1.27 (s, 18H; 6-C(CH_3)$_3$), 1.07 ppm (m, 8H; OCH$_2$$CH_2$); ^{13}C NMR (75 MHz, C_6D_6, 25 °C): δ = 168.3 (2C; C1), 149.7 (2C; C8), 145.3 (2C; C6), 138.6 (2C; C4), 136.5 (2C; C3), 118.1 (2C; C5), 104.2 (2C; C7), 69.1 (4C; OCH$_2$CH$_2$), 58.6 (1C; C_{bridge}), 35.5 (2C; 6-*C*(CH_3)$_3$), 34.7 (2C; 4-*C*(CH_3)$_3$), 32.0 (6C; 6-C(CH_3)$_3$), 31.6 (6C; 4-C(CH_3)$_3$), 25.1 ppm (4C; OCH$_2$$CH_2$); ^{15}N NMR (30 MHz, C_6D_6, 25 °C): δ = −217 ppm (s); MS (LIFDI): *m/z* (%): 532.2 (100) [M−2(THF)], 474.3 (30) [4,6-*t*BuNCOC$_6$H$_2$)$_2$CH$_2$]; elemental analysis calcd (%) for $C_{44}H_{69}ClMgN_2O_4$: C 70.48, H 9.28, N 3.74; found: C 69.30, H 8.72, N 3.81.

[Mg{(4,6-*t*Bu-NCOC$_6$H$_2$)$_2$CH}$_2$] (7), Method a: Complex **6** (228 mg, 304 μmol, 1.00 equiv) and KC_8 (41.0 mg, 304 μmol, 1.00 equiv) were suspended in toluene (15 mL) and stirred at RT for 72 h. The suspension was filtered via cannula and the solvent was removed under reduced pressure to give **7** (118 mg, 80%) as a reddish-orange solid.

Method b: Complex **6** and KC_8 were suspended in toluene (15 mL) at 0 °C then stirred for 72 h, during which time the cooling bath was allowed to slowly warm to rt. The suspension was filtered via cannula and the solvent was removed under reduced pressure to give **7** as a reddish-orange solid.

Method c: Complex **6** (300 mg, 412 μmol, 1.00 equiv) was dissolved in toluene then stirred over a potassium mirror (56.0 mg, 412 μmol, 1.00 equiv) at RT for 72 h. The suspension was filtered via cannula and the solvent was removed under reduced pressure to give **7** (152 mg, 76%) as a reddish-orange solid. ^{1}H NMR (400 MHz, [D$_{12}$]cyclohexane, 25 °C): δ = 7.05 (d, ^4J(H,H) = 2.0 Hz, 4H; H3), 7.01 (d, ^4J(H,H) = 2.0 Hz, 4H; H5), 5.38 (s, 2H; H_{bridge}), 1.25 (s, 36H; 4-C(CH_3)$_3$), 1.15 ppm (s, 36H; 6-C(CH_3)$_3$); ^{13}C NMR (100 MHz, [D$_{12}$]cyclohexane, 25 °C): δ = 168.5 (4C; C1), 150.1 (4C; C3), 145.3 (4C; C6), 138.7 (4C; C4), 136.2 (4C; C8), 118.6 (4C; C5), 104.3 (4C; C7), 60.9 (2C; C_{bridge}), 35.2 (4C; 6-*C*(CH_3)$_3$), 35.2 (4C; 4-*C*(CH_3)$_3$), 31.9 (12C; 6-C(CH_3)$_3$), 30.9 ppm (12C; 4-C(CH_3)$_3$); ^{15}N NMR (30 MHz, C_6D_6, 25 °C): δ = −213 ppm (s); MS (LIFDI): *m/z* (%): 970.7 (100) [M]; a suitable elemental analysis could not be obtained, presumably to magnesium nitride formation.

Crystallographic details

Shock-cooled crystals were selected from a Schlenk flask under an argon atmosphere by using an X-TEMP2 device.[57–59] The data were collected with an IμS microfocus source.[60] All data were integrated with the SAINT program.[61] A multiscan absorption correction (SADABS),[62] and for **3** and **6** a 3λ correction, were applied.[63] The structures were solved by direct methods (SHELXT)[64] and refined on F^2 by using the full-matrix least-squares method of SHELXL[65] within the SHELXLE GUI.[66] CCDC 1551829 (**3**), 1551830 (**4**),

Table 4. Crystallographic data for compounds **3**–**6**.

	3	**4**	**5**	**6**·pentane
formula	$C_{31}H_{42}N_2O_2$	$C_{35}H_{49}LiN_2O_3$	$C_{31}H_{41}KN_2O_2$	$C_{44}H_{69}ClMgN_2O_4$
MW [g mol^{-1}]	474.66	552.70	512.76	749.77
T [K]	100(2)	180(2)	100(2)	100(2)
space group	$P2_1/n$	$C2/c$	$P\bar{1}$	$P2_1/n$
a [Å]	18.068(2)	34.402(6)	9.242(2)	10.775(3)
b [Å]	7.992(2)	12.474(2)	9.733(2)	27.033(7)
c [Å]	19.848(2)	15.983(3)	17.430(3)	14.765(4)
α [°]	90	90	86.98(2)	90
β [°]	100.75(2)	103.89(2)	88.01(2)	90.92(2)
γ [°]	90	90	69.48(2)	90
V [Å]^3	2815.7(8)	6658(2)	1466.1(5)	4300(2)
Z	4	8	2	4
μ [mm^{-1}]	0.069	0.069	0.210	0.145
θ_{max} [°]	26.062	25.510	23.301	26.103
reflns measured	50265	49428	37614	64634
reflns unique	5570	6154	4010	8491
R_{int}	0.0564	0.0905	0.1275	0.0410
data/restr./para.	5570/1781/606	6154/1712/494	4010/712/393	8491/771/546
R_1 [$I > 2\sigma(I)$][a]	0.0436	0.0805	0.0859	0.0438
wR_2 (all)[b]	0.1055	0.2347	0.2061	0.1024
ε	0.0029(4)	–	–	–
$\Delta\rho_{fin}$ [e Å^{-3}]	0.230/−0.168	0.328/−0.351	0.378/−0.384	0.345/−0.293

[a] $R_1 = (\Sigma||F_o| - |F_c||)/(\Sigma|F_o|)$. [b] $wR_2 = [\{\Sigma w(F_o^2 - F_c^2)^2\}/\{\Sigma w(F_o^2)^2\}]^{1/2}$.

1551831 (**5**), and 1551832 (**6**·pentane) contain the supplementary crystallographic data for this paper. These data are provided free of charge by The Cambridge Crystallographic Data Centre. See Table 4 for details; additional details about the crystallographic data can be found in the Supporting Information.

Acknowledgements

Thanks to the Danish National Research Foundation (DNRF93) funded Center for Materials Crystallography (CMC) for partial support and the Federal State of Lower Saxony, Germany for providing a fellowship in the CaSuS PhD program.

Keywords: ligand design · metalation · NacNac · s-block chemistry · substituted methanides

[1] a) J. E. Parks, R. H. Holm, *Inorg. Chem.* **1968**, *7*, 1408 – 1416; b) R. Bonnett, D. C. Bradley, K. J. Fisher, *Chem. Commun.* **1968**, 886 – 887; c) D. J. Mindiola, *Angew. Chem. Int. Ed.* **2009**, *48*, 6198 – 6200; *Angew. Chem.* **2009**, *121*, 6314 – 6316.
[2] A. Stasch, C. Jones, *Dalton Trans.* **2011**, *40*, 5659 – 5672.
[3] C. Camp, J. Arnold, *Dalton Trans.* **2016**, *45*, 14462 – 14498.
[4] L. Bourget-Merle, M. F. Lappert, J. R. Severn, *Chem. Rev.* **2002**, *102*, 3031 – 3066.
[5] C. Chen, S. M. Bellows, P. L. Holland, *Dalton Trans.* **2015**, *44*, 16654 – 16670.
[6] J. Feldman, S. J. McLain, A. Parthasarathy, W. J. Marshall, J. C. Calabrese, S. D. Arthur, *Organometallics* **1997**, *16*, 1514 – 1516.
[7] M. Cheng, D. R. Moore, J. J. Reczek, B. M. Chamberlain, E. B. Lobkovsky, G. W. Coates, *J. Am. Chem. Soc.* **2001**, *123*, 8738 – 8749.
[8] M. Stender, R. J. Wright, B. E. Eichler, J. Prust, M. M. Olmstead, H. W. Roesky, P. P. Power, *J. Chem. Soc. Dalton Trans.* **2001**, 3465 – 3469.
[9] W. W. Schoeller, *Inorg. Chem.* **2011**, *50*, 2629 – 2633.
[10] P. H. M. Budzelaar, A. B. van Oort, A. G. Orpen, *Eur. J. Inorg. Chem.* **1998**, 1485 – 1494.
[11] A. L. Kenward, J. A. Ross, W. E. Piers, M. Parvez, *Organometallics* **2009**, *28*, 3625 – 3628.
[12] F. Basuli, J. C. Huffman, D. J. Mindiola, *Inorg. Chem.* **2003**, *42*, 8003 – 8010.
[13] P. P. Power, *Nature* **2010**, *463*, 171 – 177.
[14] Z. Yang, M. Zhong, X. Ma, S. De, C. Anusha, P. Parameswaran, H. W. Roesky, *Angew. Chem. Int. Ed.* **2015**, *54*, 10225 – 10229; *Angew. Chem.* **2015**, *127*, 10363 – 10367.
[15] Z. Yang, M. Zhong, X. Ma, K. Nijesh, S. De, P. Parameswaran, H. W. Roesky, *J. Am. Chem. Soc.* **2016**, *138*, 2548 – 2551.
[16] S. Harder, J. Brettar, *Angew. Chem. Int. Ed.* **2006**, *45*, 3474 – 3478; *Angew. Chem.* **2006**, *118*, 3554 – 3558.
[17] J. Spielmann, S. Harder, *Chem. Eur. J.* **2007**, *13*, 8928 – 8938.
[18] S. P. Green, C. Jones, A. Stasch, *Science* **2007**, *318*, 1754 – 1757.
[19] S. P. Green, C. Jones, A. Stasch, *Angew. Chem. Int. Ed.* **2008**, *47*, 9079 – 9083; *Angew. Chem.* **2008**, *120*, 9219 – 9223.
[20] S. J. Bonyhady, S. P. Green, C. Jones, S. Nembenna, A. Stasch, *Angew. Chem. Int. Ed.* **2009**, *48*, 2973 – 2977; *Angew. Chem.* **2009**, *121*, 3017 – 3021.
[21] S. J. Bonyhady, C. Jones, S. Nembenna, A. Stasch, A. J. Edwards, G. J. McIntyre, *Chem. Eur. J.* **2010**, *16*, 938 – 955.
[22] A. J. Boutland, I. Pernik, A. Stasch, C. Jones, *Chem. Eur. J.* **2015**, *21*, 15749 – 15758.
[23] M. S. Hill, D. J. Liptrot, C. Weetman, *Chem. Soc. Rev.* **2016**, *45*, 972 – 988.
[24] A. Steiner, D. Stalke, *J. Chem. Soc. Chem. Commun.* **1993**, 444 – 446.
[25] H. Gornitzka, D. Stalke, *Angew. Chem. Int. Ed. Engl.* **1994**, *33*, 693 – 695; *Angew. Chem.* **1994**, *106*, 695 – 698.
[26] H. Gornitzka, D. Stalke, *Organometallics* **1994**, *13*, 4398 – 4405.
[27] A. Steiner, D. Stalke, *Organometallics* **1995**, *14*, 2422 – 2429.
[28] A. Steiner, D. Stalke, *Angew. Chem. Int. Ed. Engl.* **1995**, *34*, 1752 – 1755; *Angew. Chem.* **1995**, *107*, 1908 – 1910.
[29] T. Kottke, D. Stalke, *Chem. Ber.* **1997**, *130*, 1365 – 1374.
[30] H. Gornitzka, D. Stalke, *Eur. J. Inorg. Chem.* **1998**, 311 – 317.
[31] H. Gornitzka, C. Hemmert, G. Bertrand, M. Pfeiffer, D. Stalke, *Organometallics* **2000**, *19*, 112 – 114.
[32] M. Pfeiffer, F. Baier, T. Stey, D. Leusser, D. Stalke, B. Engels, D. Moigno, W. Kiefer, *J. Mol. Model.* **2000**, *6*, 299 – 311.
[33] M. Pfeiffer, T. Stey, H. Jehle, B. Klüpfel, W. Malisch, V. Chandrasekhar, D. Stalke, *Chem. Commun.* **2001**, 337 – 338.
[34] A. Abbotto, S. Bradamante, A. Facchetti, G. A. Pagani, *J. Org. Chem.* **2002**, *67*, 5753 – 5772.
[35] P. Vasko, V. Kinnunen, J. O. Moilanen, T. L. Roemmele, R. T. Boere, J. Konu, H. M. Tuononen, *Dalton Trans.* **2015**, *44*, 18247 – 18259.
[36] D.-R. Dauer, D. Stalke, *Dalton Trans.* **2014**, *43*, 14432 – 14439.
[37] D.-R. Dauer, M. Flügge, R. Herbst-Irmer, D. Stalke, *Dalton Trans.* **2016**, *45*, 6149 – 6158.
[38] D.-R. Dauer, M. Flügge, R. Herbst-Irmer, D. Stalke, *Dalton Trans.* **2016**, *45*, 6136 – 6148.
[39] D.-R. Dauer, I. Koehne, R. Herbst-Irmer, D. Stalke, *Eur. J. Inorg. Chem.* **2017**, 1966 – 1978.
[40] H. Ben Ammar, J. Le Nôtre, M. Salem, M. T. Kaddachi, P. H. Dixneuf, *J. Organomet. Chem.* **2002**, *662*, 63 – 69.
[41] M. Arrowsmith, M. R. Crimmin, M. S. Hill, G. Kociok-Kohn, *Dalton Trans.* **2013**, *42*, 9720 – 9726.
[42] R. G. Pearson, *J. Am. Chem. Soc.* **1963**, *85*, 3533 – 3539.
[43] C. Lambert, P. von R. Schleyer, *Angew. Chem. Int. Ed. Engl.* **1994**, *33*, 1129 – 1140; *Angew. Chem.* **1994**, *106*, 1187 – 1199.
[44] W.-P. Leung, Q. W.-Y. Ip, T.-W. Lam, T. C. W. Mak, *Organometallics* **2004**, *23*, 1284 – 1291.
[45] D. Hoffmann, W. Bauer, F. Hampel, N. J. R. van Eikema Hommes, P. von R. Schleyer, P. Otto, U. Pieper, D. Stalke, D. S. Wright, R. Snaith, *J. Am. Chem. Soc.* **1994**, *116*, 528 – 536.
[46] G. Rabe, H. W. Roesky, D. Stalke, F. Pauer, G. M. Sheldrick, *J. Organomet. Chem.* **1991**, *403*, 11 – 19.
[47] A. W. Addison, T. N. Rao, J. Reedijk, J. van Rijn, G. C. Verschoor, *J. Chem. Soc. Dalton Trans.* **1984**, 1349 – 1356.
[48] D. Kratzert, D. Leusser, D. Stern, J. Meyer, F. Breher, D. Stalke, *Chem. Commun.* **2011**, *47*, 2931 – 2933.
[49] R. Neufeld, D. Stalke, *Chem. Sci.* **2015**, *6*, 3354 – 3364.

[50] S. Bachmann, R. Neufeld, M. Dzemski, D. Stalke, *Chem. Eur. J.* **2016**, *22*, 8462 – 8465.
[51] S. Bachmann, B. Gernert, D. Stalke, *Chem. Commun.* **2016**, *52*, 12861 – 12864.
[52] R. Neufeld, M. John, D. Stalke, *Angew. Chem. Int. Ed.* **2015**, *54*, 6994 – 6998; *Angew. Chem.* **2015**, *127*, 7100 – 7104.
[53] Virtuelles Labor I, http://www.stalke.chemie.uni-goettingen.de/ virtuelles labor/advanced/13 de.html.
[54] W. Uhlig, *Z. Naturforsch. B* **1995**, *50*, 1674 – 1678.
[55] R. Neufeld, T. L. Teuteberg, R. Herbst-Irmer, R. A. Mata, D. Stalke, *J. Am. Chem. Soc.* **2016**, *138*, 4796 – 4806.
[56] Virtuelles Labor II, http://www.stalke.chemie.uni-goettingen.de/virtuelles labor/nmr/de.html.
[57] T. Kottke, D. Stalke, *J. Appl. Crystallogr.* **1993**, *26*, 615 – 619.
[58] D. Stalke, *Chem. Soc. Rev.* **1998**, *27*, 171 – 178.
[59] Virtuelles Labor III, http://www.stalke.chemie.uni-goettingen.de/virtuelleslabor/special/22de.html.
[60] T. Schulz, K. Meindl, D. Leusser, D. Stern, J. Graf, C. Michaelsen, M. Ruf, G. M. Sheldrick, D. Stalke, *J. Appl. Crystallogr.* **2009**, *42*, 885 – 891.
[61] Bruker AXS Inc., in *Bruker Apex CCD*, *SAINT v8.30C* (Ed.: Bruker AXS Inst. Inc.), WI, USA, Madison, **2013**.
[62] L. Krause, R. Herbst-Irmer, G. M. Sheldrick, D. Stalke, *J. Appl. Crystallogr.* **2015**, *48*, 3 – 10.
[63] L. Krause, R. Herbst-Irmer, D. Stalke, *J. Appl. Crystallogr.* **2015**, *48*, 1907 – 1913.
[64] G. M. Sheldrick, *Acta Crystallogr. Sect. A* **2015**, *71*, 3 – 8.
[65] G. M. Sheldrick, *Acta Crystallogr. Sect. C* **2015**, *71*, 3 – 8.
[66] C. B. Hübschle, B. Dittrich, *J. Appl. Crystallogr.* **2011**, *44*, 238 – 240.

Manuscript received: May 24, 2017
Version of record online: ■■ ■■, 0000

FULL PAPER

Metal–Ligand Complexes

*I. Koehne, S. Bachmann, T. Niklas, R. Herbst-Irmer, D. Stalke**

■■ – ■■

A Novel Bulky Heteroaromatic-Substituted Methanide Mimicking NacNac: Bis(4,6-*tert*-butylbenzoxazol-2-yl)methanide in s-Block Metal Coordination

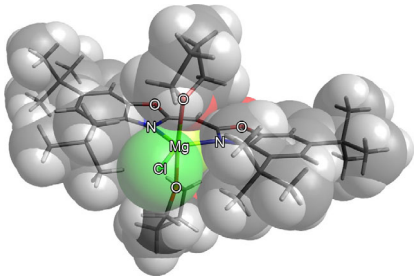

NacNac mimic: Metalation of the methylene bridging moiety in a novel bulky bis(4,6-*t*Bu-benzoxazol-2-yl)methanide ligand with s-block organometallic reagents gave the corresponding N,N-chelated metal salts. Structural features in the solid state (see figure) and in solution were compared to related complexes derived from the ubiquitous NacNac ligand.